

# A new Phenol Red-modified porphyrin as efficient protein photocleaving agent†

Guo-Yu Jiang,<sup>ab</sup> Wan-Hua Lei,<sup>a</sup> Qian-Xiong Zhou,<sup>ab</sup> Yuan-Jun Hou,<sup>a</sup>  
Xue-Song Wang\*<sup>a</sup> and Bao-Wen Zhang\*<sup>a</sup>

Received 24th March 2010, Accepted 24th June 2010

DOI: 10.1039/c0cp00012d

Protein affinity is of importance for porphyrins in their application in photodynamic therapy (PDT). A new Phenol Red-modified porphyrin (R-TPP) was designed and synthesized to fully take advantage of the binding character of Phenol Red towards protein. Detailed comparisons of absorption spectra, fluorescence spectra, n-octanol/water partition coefficients, <sup>1</sup>O<sub>2</sub> quantum yields, as well as protein photocleaving abilities between R-TPP and its parent porphyrin Br-TPP clearly demonstrate the benefits stemming from the modification of Phenol Red. On one hand, the presence of Phenol Red moiety greatly enhances the binding affinity of R-TPP towards model proteins (bovine serum albumin and hen egg lysozyme), and therefore improves the availability of <sup>1</sup>O<sub>2</sub>. On the other hand, the presence of Phenol Red moiety provides R-TPP with amphiphilic character, and therefore restricts aggregation and favors the generation of <sup>1</sup>O<sub>2</sub>. As a result, R-TPP photocleaves proteins efficiently, showing promising application potential in PDT.

## Introduction

Photodynamic therapy (PDT) is a dual-selective medicinal treatment, which combines light and a photosensitizer to bring about cytotoxic effects to cancer cells.<sup>1</sup> Among the different types of photosensitizers being used in PDT, porphyrins are the most extensively studied, and several of them have gained approval for clinical use.<sup>1</sup> The porphyrin-based PDT mainly relies on the singlet oxygen (<sup>1</sup>O<sub>2</sub>) production. <sup>1</sup>O<sub>2</sub> is a highly reactive species, however, has a very short lifetime in biological systems (<0.04 μs) and therefore, a very limited diffusion range in tumor cells (<0.02 mm),<sup>2</sup> implying the importance of the binding ability of porphyrins towards <sup>1</sup>O<sub>2</sub> biotarget. Intracellular proteins are expected to be the major targets of <sup>1</sup>O<sub>2</sub>, due to their abundance within cells (ca. 70% of the dry mass of most cells) and their high reaction rate constants with <sup>1</sup>O<sub>2</sub>.<sup>3</sup> The oxidative damage to proteins can regulate cellular signaling events, including apoptosis.<sup>4</sup> In this regard, protein-binding ability is of importance in development of new porphyrins for PDT application. On the other hand, serum albumin is known to be the most abundant circulatory protein and can accumulate in malignant and inflamed tissue due to a leaky capillary combined with an absence or defective lymphatic drainage system and thus is emerging as a versatile targeting carrier for drugs, including PDT agents.<sup>5,6</sup> Accordingly, protein affinity may also benefit tumor targeting of porphyrins by aiding their coupling to either endogenous or exogenous serum albumin. Additionally, porphyrins possessing

protein binding capability may be useful for structure–activity studies of proteins by spatio-temporal control of protein cleavage.<sup>7</sup>

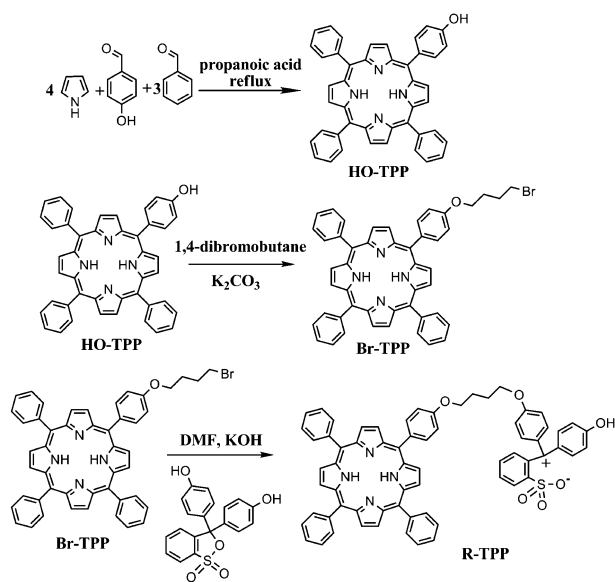
The important role of protein-binding in porphyrin-based PDT agents inspired extensive studies on the interactions between porphyrins and proteins,<sup>8</sup> mainly bovine serum albumin (BSA), a serum protein that not only is the most common model protein but also has been utilized in targeting delivery of phototherapeutic sensitizers.<sup>9</sup> However, just recently, efforts are emerging to pursue novel porphyrins with high protein affinity by intended structure design.<sup>10</sup> For example, Anzenbacher<sup>10a</sup> introduced phosphonate groups to modulate the binding of the corresponding porphyrins to BSA. Yano<sup>10b</sup> found that the binding numbers of the glyco-conjugated porphyrins to BSA depended on the sugar moieties. Only Toshima<sup>10c</sup> clearly disclose, for the first time, that 5,10,15,20-tetra(4-hydroxyphenyl) porphyrin effectively and selectively degraded the target transcription factor, human estrogen receptor-α (hER-α), upon visible light irradiation, due to the similarity of its structure to an estradiol, which has high affinity for hER.

Phenol Red is a commonly used pH indicator which belongs to the well known triarylmethane dyes. It is used in biology to estimate the physiological function of the kidney and for colorimetric or spectrophotometric determination of blood or plasma pHs.<sup>11</sup> It is also used as a pH indicator in tissue culture media. Phenol Red was known to be able to bind to BSA, with a binding constant of  $1.1 \times 10^5 \text{ M}^{-1}$ .<sup>12</sup> Taking advantage of the protein-binding character of Phenol Red, herein, we designed and synthesized a porphyrin-Phenol Red conjugate (R-TPP, Scheme 1), expecting that the Phenol Red moiety may enhance the binding of the porphyrin with proteins. UV-visible absorption, fluorescence emission, time-resolved absorption spectra, and protein photocleavage measurements indeed show an improved protein affinity of

<sup>a</sup> Key Laboratory of Photochemical Conversion and Optoelectronic Materials, Technical Institute of Physics and Chemistry, Chinese Academy of Sciences, Beijing 100190, P. R. China.  
E-mail: xswang@mail.ipc.ac.cn, g203@mail.ipc.ac.cn

<sup>b</sup> Graduate School of Chinese Academy of Sciences, Beijing 100049

† Electronic supplementary information (ESI) available: NMR and HRMS spectra. See DOI: 10.1039/c0cp00012d



Scheme 1 Synthetic route of R-TPP.

R-TPP towards two model proteins, both BSA and hen egg lysozyme (Lyso). As a result, R-TPP can effectively photocleave BSA and Lyso.

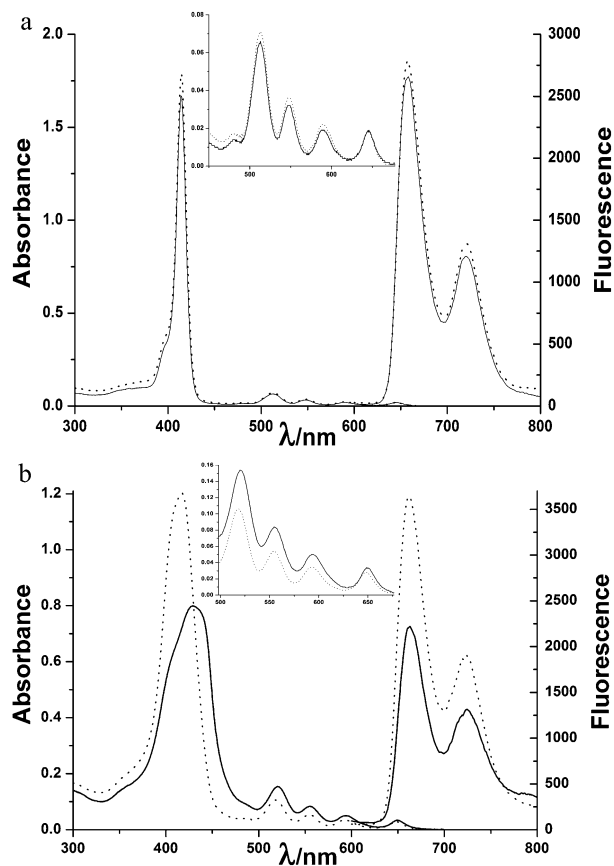


Fig. 1 The absorption and emission spectra ( $\lambda_{\text{ex}} = 415$  nm in CH<sub>3</sub>CN, and  $\lambda_{\text{ex}} = 420$  nm in PBS/DMSO) of Br-TPP (solid lines) and R-TPP (dotted lines) in CH<sub>3</sub>CN (a) and in PBS/DMSO (3:1 in volume ratio) (b). Insets show the expanded spectra of the Q-bands.

## Results and discussion

### Synthesis of a Phenol Red modified porphyrin (R-TPP)

HO-TPP was prepared by condensation of pyrrole, benzaldehyde and 4-hydroxybenzaldehyde in refluxing propanoic acid. Br-TPP was prepared from the reaction of HO-TPP and 1,4-dibromobutane in the presence of potassium carbonate. R-TPP was prepared from Br-TPP and Phenol Red in a similar procedure, using potassium hydroxide instead of potassium carbonate (Scheme 1).

### Photophysical and photochemical properties of the examined porphyrins

Fig. 1a shows the absorption and emission spectra ( $\lambda_{\text{ex}} = 415$  nm) of the two porphyrins, Br-TPP and R-TPP, in acetonitrile and Table 1 lists the corresponding spectra data. The spectra data of the two porphyrins in CH<sub>2</sub>Cl<sub>2</sub> are also included in Table 1. Both Br-TPP and R-TPP show typical UV-Vis spectra of free base porphyrins, with one intense peak (Soret band) at *ca.* 415 nm and four vibronic peaks (Q bands) at *ca.* 513, 547, 590 and 645 nm, respectively. The emission spectra of the two porphyrins in acetonitrile are quite similar too, showing the fine structures peaked at about 660 nm and 720 nm. The fluorescence quantum yields of Br-TPP and R-TPP in the three examined solvents were measured using TMPyP as reference, whose fluorescence quantum yield was reported to be 0.017 in PBS.<sup>13</sup> The high extent of similarity in absorption spectra, emission spectra, as well as fluorescence quantum yields of Br-TPP and R-TPP indicates the lack of intramolecular interactions between porphyrin and Phenol Red moieties in both ground and singlet excited state of R-TPP.

Since the application of the photodynamic properties of porphyrins is in aqueous solutions, the photophysical and photochemical properties of Br-TPP and R-TPP were also compared in PBS. Due to the poor solubility of Br-TPP in aqueous solution, a PBS/DMSO (3:1 in volume ratio) mixed solution was used in our studies. The absorption and emission spectra ( $\lambda_{\text{ex}} = 420$  nm) of Br-TPP and R-TPP in aqueous solutions are shown in Fig. 1b. Obviously, the Soret bands of both porphyrins in PBS became red-shifted and much broader compared to those in acetonitrile (Table 1), which implies the aggregation of the two porphyrins in aqueous solutions. For Br-TPP this broadening is more remarkable, in line with its highly hydrophobic character. The *n*-octanol/water partition coefficients of Br-TPP and R-TPP were measured to be 2.17 and 0.12, respectively (Table 2), fully demonstrating the capability of the Phenol Red moiety in making a hydrophobic photosensitizer become an amphiphilic. It is well accepted that amphiphilicity is of importance for an ideal PDT photosensitizer.<sup>14</sup> The aggregation behavior of Br-TPP and R-TPP may also partly account for their much lower fluorescence quantum yields in PBS than in acetonitrile (Table 1).

The <sup>1</sup>O<sub>2</sub> production abilities of the two porphyrins in acetonitrile were evaluated by measuring the degradation rate of 1,3-diphenylisobenzofuran (DPBF) (Scheme 2) by <sup>1</sup>O<sub>2</sub> generated upon photoirradiation and using 5,10,15,20-tetra-phenyl porphyrin (TPP) as reference (Fig. 2a, Table 2). The <sup>1</sup>O<sub>2</sub> quantum yield of R-TPP is as high as that of Br-TPP,

**Table 1** Photophysical properties of Br-TPP and R-TPP in CH<sub>2</sub>Cl<sub>2</sub>, CH<sub>3</sub>CN (5 μM) and in aqueous solutions (10 μM)

	Solvent	$\lambda_{\text{max}}/\text{nm}$ ( $\epsilon \times 10^{-3}/\text{M}^{-1} \text{cm}^{-1}$ )				$\lambda_{\text{em}}/\text{nm}$		Fluorescence quantum yield
		Soret band	Q bands					
Br-TPP	CH <sub>2</sub> Cl <sub>2</sub>	418.0	515.5	550.5	590.5	645.5	720.4	0.023
		(265.0)	(10.6)	(5.2)	(3.4)	(2.8)		
	CH <sub>3</sub> CN	414.0	513.0	547.5	589.5	644.5	719.6	0.033
		(343.4)	(23.0)	(16.2)	(13.6)	(13.6)		
R-TPP	CH <sub>3</sub> CN	429.0	520.0	555.0	593.5	650.0	724.2	0.0085
		(80.0)	(15.4)	(8.4)	(5.0)	(3.4)		
	CH <sub>2</sub> Cl <sub>2</sub>	418.0	515.5	550.5	592.0	646.0	721.0	0.021
		(288.2)	(11.4)	(5.8)	(3.4)	(2.6)		
R-TPP	CH <sub>3</sub> CN	414.5	512.5	547.5	590.0	645.0	721.2	0.034
		(365.4)	(21.8)	(14.8)	(12.0)	(11.4)		
	PBS <sup>a</sup>	417.5	519.5	554.5	592.0	648.0	724.0	0.0095
		(60.0)	(10.7)	(2.5)	(1.5)	(1.2)		

<sup>a</sup> Due to the poor solubility of Br-TPP in aqueous solution, a PBS/DMSO (3:1 in volume ratio) was used.

**Table 2** Singlet oxygen quantum yields ( $\Phi_{\Delta}$ ) in CH<sub>3</sub>CN, n-octanol/water partition coefficients ( $\log P$ ) and triplet excited state lifetimes of Br-TPP and R-TPP

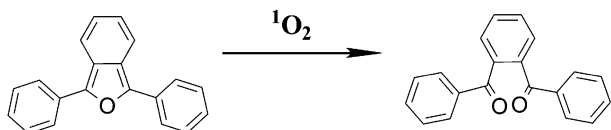
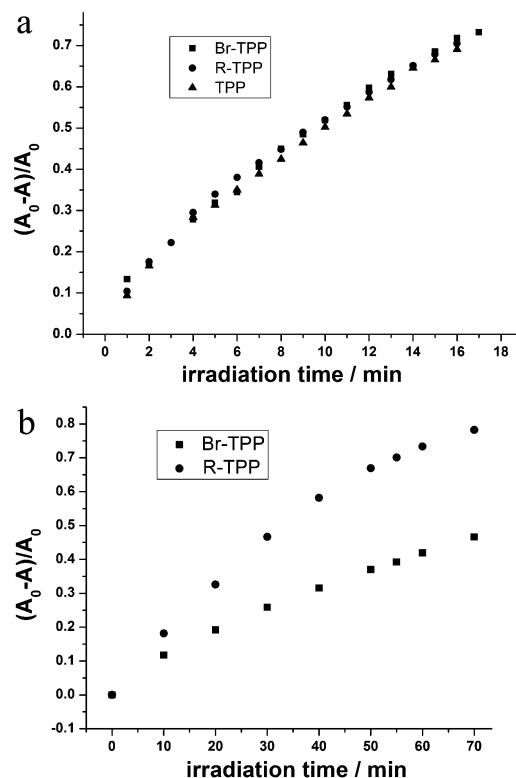
	Br-TPP	R-TPP
$\Phi_{\Delta}$ <sup>a</sup>	0.59	0.59
$\log P$ <sup>b</sup>	2.17	0.12
$\tau_T$ <sup>c</sup> /μs	4.2	3.8

<sup>a</sup> TPP in acetonitrile was used as reference (0.60). <sup>b</sup> SD < 5%.  
<sup>c</sup> In CH<sub>3</sub>CN.

suggesting that no intramolecular interactions between porphyrin and Phenol Red moieties in the triplet excited state of R-TPP. The similar triplet excited state lifetimes of Br-TPP and R-TPP also support this conclusion (Table 2).

The singlet oxygen production abilities of Br-TPP and R-TPP were also compared in PBS by measuring the degradation rate of 9,10-anthracenediylbis(methylene)dimalonic acid (AMDA) (Scheme 3, Fig. 2b). Though both porphyrins exhibit the same <sup>1</sup>O<sub>2</sub> quantum yield in CH<sub>3</sub>CN, in aqueous solutions, Br-TPP showed much lower <sup>1</sup>O<sub>2</sub> generation ability than R-TPP, most likely originating from its lower water solubility and thus higher aggregation extent.

The spin trapping technique was also used to confirm the production of <sup>1</sup>O<sub>2</sub> and other reactive oxygen species, such as hydroxyl radical (Fig. 3). Upon irradiation of oxygen-saturated PBS (5 mM, pH = 7.0)/DMSO (3:1 in volume ratio) of R-TPP (1mM) and 2,2,6,6-tetramethyl-4-piperidone (TEMPO) (50 mM) with 532 nm laser, a three-line EPR spectrum with equal intensity and hyperfine coupling constant of  $a_N = 16.0$  G was observed which could be assigned to the TEMPO (TEMP-<sup>1</sup>O<sub>2</sub> adduct) signal. However, when 5,5-dimethyl-1-pyrroline-*N*-oxide (DMPO) was used as the <sup>•</sup>OH trap in the same experimental conditions, no ESR signal was observed

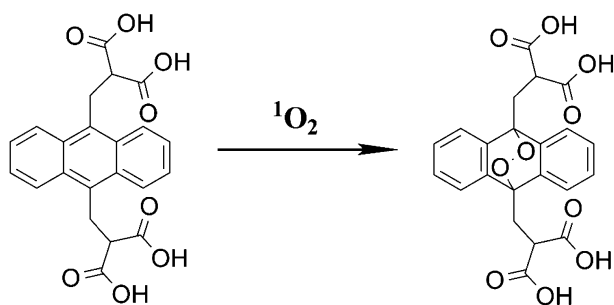
**Scheme 2** Reaction of DPBF with singlet oxygen (<sup>1</sup>O<sub>2</sub>).**Fig. 2** Degradation of DPBF (a) and AMDA (b) by <sup>1</sup>O<sub>2</sub> generated by Br-TPP and R-TPP upon irradiation.

after irradiation, indicating that R-TPP did not have the ability to generate <sup>•</sup>OH.

### Protein photocleavage

Protein electrophoresis experiments were carried out to investigate the protein photocleaving abilities of Br-TPP and R-TPP, using both BSA and Lyso as model proteins (Fig. 4).

Br-TPP exhibited very weak photocleavage ability towards both BSA and Lyso (lane 2). In stark contrast, R-TPP led to significant photocleavage of BSA and Lyso at the concentration of 25 μM (lane 4). The photocleavage was either not observed or greatly diminished in the dark or in the presence of NaN<sub>3</sub>,



**Scheme 3** Reaction of AMDA with singlet oxygen ( $^1\text{O}_2$ ) in acetonitrile.

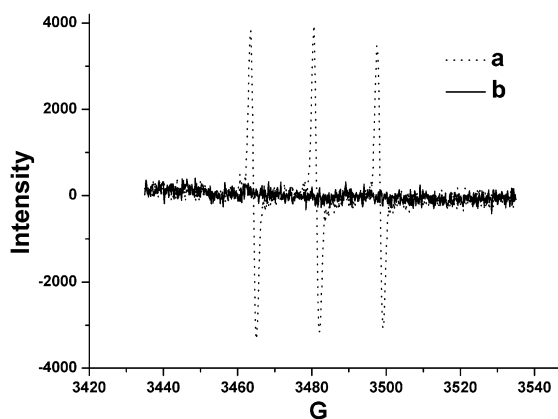


**Fig. 3** EPR signal of R-TPP (1 mM) in PBS (5 mM, pH = 7.0)/DMSO (3:1 in volume ratio) upon irradiation with 532 nm laser: (a) in the presence of 50 mM TEMP; and (b) in the presence of 50 mM DMPO.

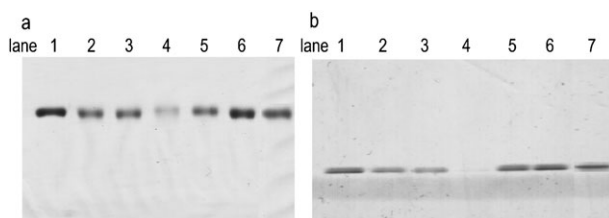


**Fig. 4** Photo-cleavage of BSA (a, 2  $\mu\text{M}$ ) and Lyso (b, 5  $\mu\text{M}$ ) in PBS (5 mM, pH = 7.0)/DMSO (3:1 in volume ratio) upon 3 h of irradiation of a broadband light (> 550 nm) and analyzed by 8% SDS-PAGE: lane 1, protein alone; lane 2, protein + Br-TPP; lane 3, protein + Br-TPP + Phenol Red (25  $\mu\text{M}$ ); lane 4, protein + R-TPP; lane 5, protein + R-TPP + excess Phenol Red; lane 6, protein + R-TPP, but without light; lane 7, protein + R-TPP +  $\text{NaN}_3$  (0.1 M). The concentrations of Br-TPP and R-TPP were fixed at 25  $\mu\text{M}$ .

indicative of the involvement of  $^1\text{O}_2$  (lane 6 and 7). The presence of 25  $\mu\text{M}$  of Phenol Red did not improve the photocleavage ability of Br-TPP (lane 3), indicating that Phenol Red itself cannot result in protein cleavage under experimental conditions and the attachment of Phenol Red onto porphyrin is critical for the observation of improved photocleavage. R-TPP possesses higher  $^1\text{O}_2$  generation efficiency in aqueous solutions than Br-TPP, undoubtedly facilitating the photocleavage of proteins. Additionally, the

targeting property of Phenol Red may also play an important role in the protein photocleavage by R-TPP. To examine this possibility, control experiment as shown in lane 5 was carried out. The addition of excess amount of Phenol Red can greatly inhibit the photocleavage of both proteins. This finding may be reasonably explained by the competitive binding of R-TPP and Phenol Red towards BSA or Lyso, as a result, the displacement of the bound R-TPP by Phenol Red decreases the availability of  $^1\text{O}_2$  in light of the short lifetime character of  $^1\text{O}_2$ .

### Binding of porphyrins towards BSA or Lyso

In order to disclose the role of Phenol Red in the much improved protein photocleavage activity of R-TPP, we investigated the binding properties of Br-TPP and R-TPP towards both BSA and Lyso.

The addition of increasing aliquots of BSA or Lyso to the PBS solutions of the two porphyrins resulted in obvious changes in decrease in the emission intensity (Fig. 5a). The addition of Lyso into Br-TPP gave similar results, *i.e.* a 4.5 nm red shift and a 16% hypochromic effect in the Soret band and a 35% reduction in the emission intensity (Fig. 5c). In the case of R-TPP, no significant red shift or hypochromicity in the Soret band was observed upon the addition of either BSA or Lyso, while the fluorescence intensity underwent a remarkable increase rather than decrease, 95% increase for BSA and 30% increase for Lyso (Fig. 5b and d). The remarkably varied water solubilities of Br-TPP and R-TPP may be responsible for the markedly different effects of the proteins. Due to the highly hydrophobic character of Br-TPP, the presence of protein may further promote its aggregation inside the hydrophobic pockets, *i.e.*, the hydrophobic pocket of the protein may trap two or more Br-TPP molecules simultaneously, thus leading to the red shift and hypochromic effect of the Soret band and fluorescence quenching. This will not occur for R-TPP due to its amphiphilic feature. Contrarily, the binding of R-TPP towards proteins may favor the monomerization of R-TPP, and enhance the fluorescence intensity. The enhancement of the fluorescence intensity of water soluble porphyrins upon addition of BSA were also found in the literature.<sup>15</sup> Consequently, the binding of Br-TPP towards proteins promotes aggregation and has a negative effect for  $^1\text{O}_2$  generation and protein cleavage, while the binding of R-TPP towards proteins restricts aggregation and exhibits a positive effect for  $^1\text{O}_2$  generation and protein cleavage.

The binding of porphyrins towards proteins not only influences the photophysical properties of porphyrins as mentioned above, but also varies the photophysical characters of proteins, *e.g.* quenches the fluorescence emission of proteins, from which both the binding mode and binding strength can be deduced. As shown in Fig. 6, the presence of R-TPP quenched the intrinsic fluorescence of both BSA and Lyso significantly, while Br-TPP quenched the protein fluorescence with a lower efficiency.

The fluorescence quenching rate constants can be calculated based on the Stern–Volmer equation (eqn (1)),<sup>16</sup> where  $k_q$ ,  $\tau_0$ , and  $[\text{Q}]$  are the fluorescence quenching rate constant, the fluorescence lifetime of protein in the absence of the quencher,

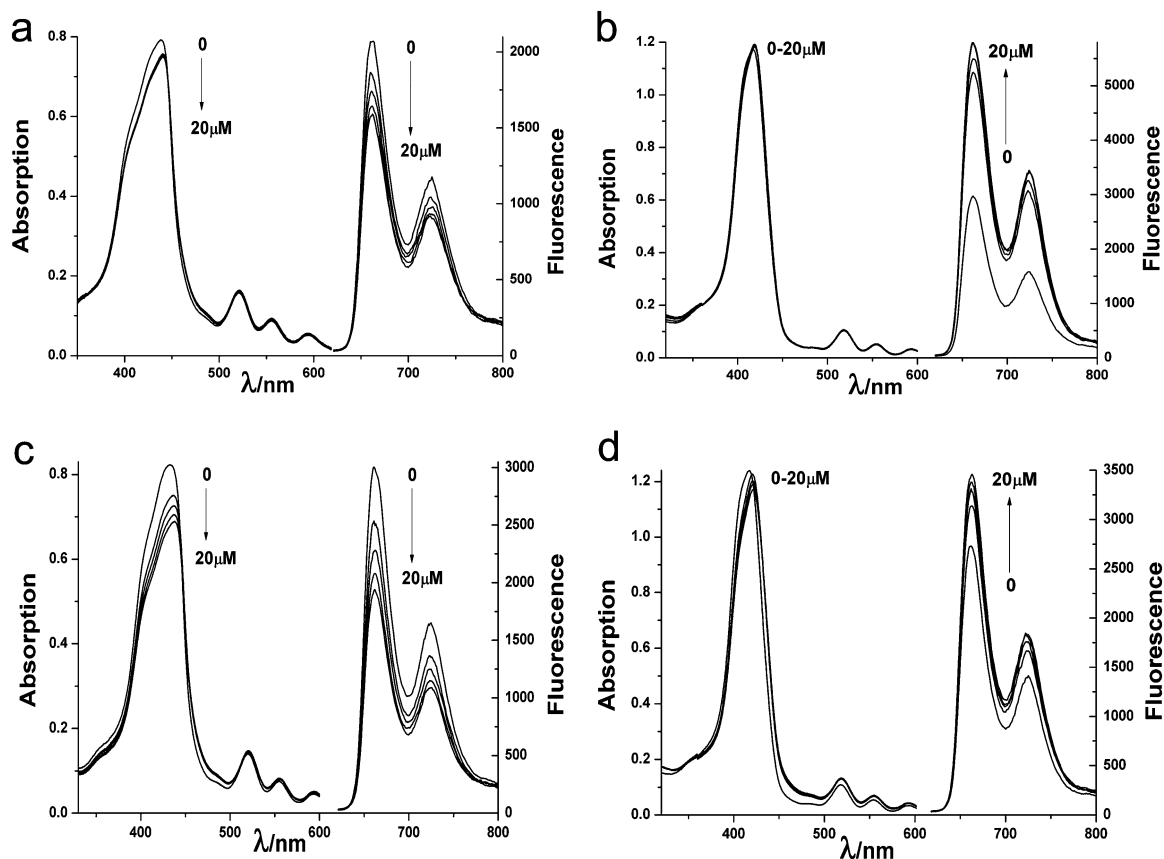


**Fig. 5** Absorption and emission spectra of Br-TPP and R-TPP (10  $\mu\text{M}$ ) in PBS/DMSO (3:1 in v/v) upon addition of increasing amounts of protein. a: Br-TPP + BSA; b: R-TPP + BSA; c: Br-TPP + Lyso; d: R-TPP + Lyso.

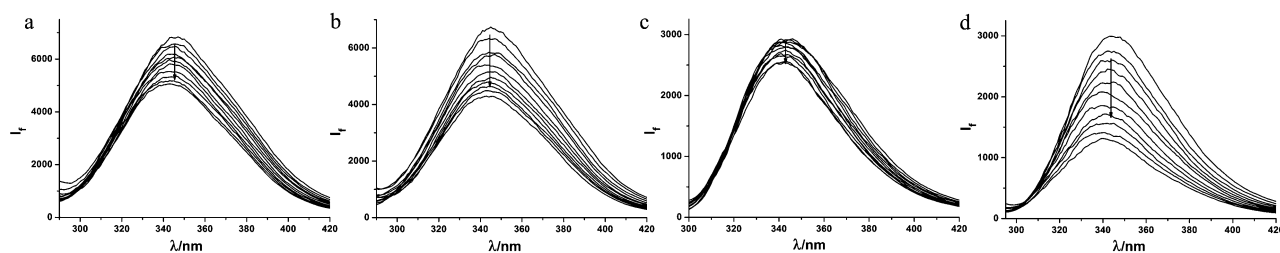


**Fig. 6** Fluorescence quenching ( $\lambda_{\text{ex}} = 280 \text{ nm}$ ) of BSA (2  $\mu\text{M}$ ) or Lyso (2  $\mu\text{M}$ ) by porphyrins (0–5  $\mu\text{M}$ ). (a) BSA + Br-TPP; (b) BSA + R-TPP; (c) Lyso + Br-TPP; (d) Lyso + R-TPP.

and the concentration of the quencher, respectively.  $F_0$  and  $F$  are the fluorescence intensities in the absence and presence of the quencher, respectively.

$$F_0/F = 1 + k_q\tau_0[Q] \quad (1)$$

Using the corrected fluorescence intensity data and the lifetime of  $10^{-8}$  s for BSA,<sup>17</sup> the quenching rate constants of Br-TPP and R-TPP are calculated to be  $3.36 \times 10^{12}$  and  $1.43 \times 10^{13} \text{ M}^{-1} \text{ s}^{-1}$ , respectively, from the slopes of the corresponding Stern–Volmer plots (Fig. 7). Since the quenching rate constants are 2–3 orders of magnitude higher than the collision quenching constant ( $2.0 \times 10^{10} \text{ M}^{-1} \text{ s}^{-1}$ )<sup>17</sup> for various quenchers with biomolecules, a static quenching mechanism,

*i.e.* the binding of Br-TPP and R-TPP towards BSA, can be concluded.

$$\left(\frac{F_0 - F}{F - F_\infty}\right) = \left(\frac{[\text{Porphyrin}]}{K_d}\right)^n \quad (2)$$

The binding constants ( $K_b$ ) can be obtained according to eqn (2),<sup>8g</sup> in which  $K_d$  is the dissociation constant ( $1/K_b$ ),  $n$  is the number of porphyrin molecules bound to each protein molecule,  $F_0$  and  $F$  are the corrected fluorescence of protein in the absence or presence of porphyrin,  $F_\infty$  is the fluorescence at infinite concentration of porphyrin (calculated as the intercept of  $1/(F_0 - F)$  vs.  $1/[\text{Porphyrin}]$ ). The plot of  $\log [(F_0 - F)/(F - F_\infty)]$  versus  $\log[\text{porphyrin}]$  yields the number of binding sites and the

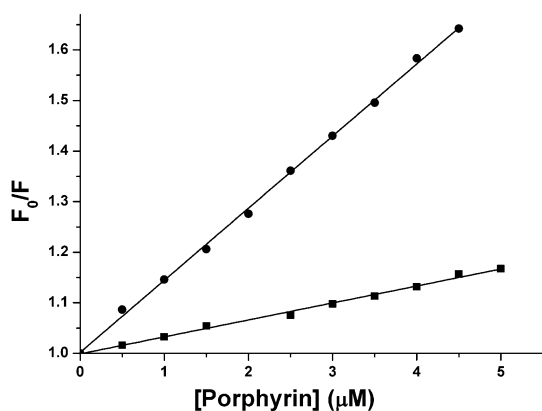


Fig. 7 Stern–Volmer plot of the BSA fluorescence quenching by Br-TPP (square) and R-TPP (circle).

value of  $K_b$  (Fig. 8 and Table 3). Clearly, the attachment of Phenol Red moiety greatly enhances the binding affinity of the corresponding porphyrin, R-TPP, than its parent porphyrin, Br-TPP.

## Conclusions

In summary, we synthesized a Phenol Red modified porphyrin, R-TPP. Compared to its parent porphyrin, Br-TPP, R-TPP exhibits two distinct advantages. At first, the presence of Phenol Red moiety greatly enhances the binding affinity of R-TPP towards proteins (BSA and Lyso), and therefore

improves the availability of  $^1\text{O}_2$  towards proteins, the major biotarget of  $^1\text{O}_2$  in PDT. Secondly, the presence of Phenol Red moiety renders R-TPP amphiphilic character, and therefore restricts aggregation and favors  $^1\text{O}_2$  generation. As a result, R-TPP can photocleave proteins efficiently, showing promising application potential in PDT.

## Experimental

### General remarks

$^1\text{H}/^{13}\text{C}$  NMR spectra were obtained on a Bruker DMX-400 MHz spectrophotometer. High resolution mass spectra were obtained on a Bruker APEX IV FT\_MS. UV-Vis absorption spectra and fluorescence emission spectra were recorded on a Shimadzu UV-1601PC spectrophotometer and a Hitachi F-4500 fluorescence spectrophotometer, respectively.

### Materials

Pyrrole, benzaldehyde, 4-hydroxybenzaldehyde, 1,4-dibromobutane, Phenol Red, 1,3-diphenylisobenzofuran (DPBF), 9,10-anthracenediyl-bis(methylene)dimalonic acid (AMDA), sodium azide ( $\text{NaN}_3$ ), 5,5-dimethyl-1-pyrroline-*N*-oxide (DMPO), 2,2,6,6-tetramethyl-4-piperidone (TEMP) and trishydroxymethylaminomethane (Tris base) were purchased from Sigma-Aldrich. All other chemicals of analytical grade were from Beijing Chemical Plant. Water is freshly distilled twice before use. Stock solutions of photosensitizers were dissolved in DMSO and kept in freezer ( $4^\circ\text{C}$ ) until use. BSA and Lyso were purchased from Sigma Aldrich.

### Synthesis of porphyrins

Synthetic route of R-TPP is shown in Scheme 1.

#### 5-(4'-Hydroxyphenyl)-10,15,20-triphenylporphyrin (HO-TPP).

HO-TPP was synthesized according to a reported method,<sup>18</sup> by reacting 4-hydroxybenzaldehyde (1.83 g, 15 mM), benzaldehyde (4.57 mL, 45 mM), and pyrrole (4.15 mL, 60 mM), in refluxing propanoic acid. The crude product was purified on a silica gel column with chloroform as eluent. Yield 10%.  $^1\text{H-NMR}$  (400 MHz in  $\text{CDCl}_3$ ),  $\delta$  ppm: 8.88 (m, 8 H), 8.23 (m, 6 H), 7.78 (m, 9 H), 8.07 (d, 2 H,  $J = 8.28$  Hz), 7.17 (d, 2 H,  $J = 8.08$  Hz),  $-2.75$  (s, 2 H).

#### 5-(4'-Bromobutoxyphenyl)-10,15,20-triphenylporphyrin (Br-TPP).

Br-TPP was synthesized by reacting HO-TPP with an excess of 1,4-dibromobutane in the presence of potassium carbonate at  $150^\circ\text{C}$  for 24 h. Crude Br-TPP was purified on a silica gel column with chloroform–ethanol (100:2 in v/v) as eluent. Yield 85%.  $^1\text{H NMR}$  (400 MHz in  $\text{CDCl}_3$ ),  $\delta$  ppm: 8.87 (m, 8 H), 8.22 (m, 6 H), 7.78 (m, 9 H), 8.13 (d, 2 H,  $J = 8.40$  Hz), 7.28 (d, 2 H,  $J = 8.88$  Hz), 4.31 (t, 2 H,  $J = 11.80$  Hz), 3.65 (t, 2 H,  $J = 13.00$  Hz), 2.26 (d, 2 H,  $J = 7.68$  Hz), 2.17 (d, 2 H,  $J = 8.04$  Hz),  $-2.75$  (s, 2 H).

#### Synthesis of the porphyrin-Phenol Red conjugate (R-TPP).

R-TPP was synthesized by reacting Br-TPP and an excess of Phenol Red in DMF in the presence of potassium hydroxide at  $150^\circ\text{C}$  for 24 h. Crude R-TPP was purified on a silica gel column with chloroform–ethanol (100:10, v/v) as eluent.

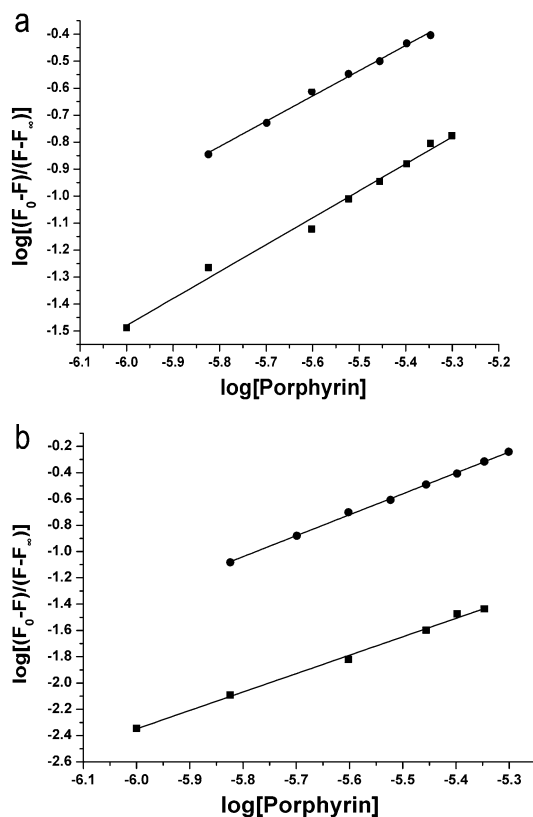


Fig. 8 Double logarithmic plots of BSA (a) and Lyso (b) fluorescence quenching by Br-TPP (square) and R-TPP (circle).

**Table 3** Binding constants of Br-TPP and R-TPP towards BSA and Lyso

	Br-TPP + BSA	R-TPP + BSA	Br-TPP + Lyso	R-TPP + Lyso
<i>n</i>	0.99	0.99	1.40	1.59
<i>K<sub>b</sub></i> /M <sup>-1</sup>	3.32 × 10 <sup>4</sup>	8.49 × 10 <sup>4</sup>	2.11 × 10 <sup>4</sup>	1.40 × 10 <sup>5</sup>

Yield 15%. <sup>1</sup>H NMR (400 MHz in CDCl<sub>3</sub>), δ ppm: 8.70 (m, 8H), 8.03 (m, 6H), 7.55–7.42 (m, 9 H), 7.79 (d, 2 H, *J* = 6.56 Hz), 6.99 (d, 2 H, *J* = 6.96 Hz), 7.08–6.52 (m, 12 H), 3.65 (s, br, 4 H), 1.26 (s, br, 4 H), –2.75 (s, 2 H). <sup>13</sup>C NMR (400 MHz in CDCl<sub>3</sub>), δ ppm: 188.2, 161.1, 158.7, 142.2, 135.6, 134.6, 131.5, 131.1, 129.9, 129.4, 127.7, 126.7, 120.2, 114.4, 112.7, 67.7, 67.5, 29.9, 26.1. HRMS, *m/z*: calculated for (M + H) = 1039.3524, found: 1039.3486.

### Fluorescence quantum yield

The fluorescence quantum yields of the synthesized porphyrins, Br-TPP and R-TPP, were evaluated using 5,10,15,20-tetrakis-(4-*N*-methylpyridyl)porphyrin (TMPyP) as reference, whose fluorescence quantum yield was reported to be 0.017 in PBS.<sup>13</sup>

In all cases, the absorbance of the sample and the reference solutions were kept below 0.1 at the excitation wavelength to minimize inner filter effects. Eqn (3) was applied to calculate the fluorescence quantum yields of the porphyrins, where *Q*, *I*, OD, *n* and *Q<sub>R</sub>*, *I<sub>R</sub>*, OD<sub>R</sub>, *n<sub>R</sub>*, are the fluorescence quantum yields, the area of the emission spectra, the optical densities and the refractive indexes of the solutions for the examined porphyrin and the reference, respectively.

$$Q = Q_R \frac{I \text{ OD}_R n^2}{I_R \text{ OD } n_R^2} \quad (3)$$

### Singlet oxygen (<sup>1</sup>O<sub>2</sub>) quantum yield

The reaction of <sup>1</sup>O<sub>2</sub> with DPBF<sup>19a</sup> (Scheme 2) was adopted to measure the <sup>1</sup>O<sub>2</sub> quantum yields of the synthesized porphyrins, using tetraphenylporphyrin (TPP) as the reference, whose <sup>1</sup>O<sub>2</sub> quantum yield was measured<sup>19b</sup> to be 0.60 in air-saturated CH<sub>3</sub>CN. A series of 2 mL of air-saturated acetonitrile solutions containing DPBF and porphyrins, of which the absorbance at 512 nm originating from the absorption of the examined porphyrin was adjusted to the same (OD<sub>512nm</sub> = 0.15), were separately charged into an opened 1 cm path fluorescence cuvette and illuminated with the light of 512 nm (obtained from a Hitachi F-4500 fluorescence spectrophotometer). The consumption of DPBF was followed by monitoring its fluorescence intensity decrease at the emission maximum (λ<sub>ex</sub> = 440 nm, λ<sub>em</sub> = 479 nm).

The reaction of <sup>1</sup>O<sub>2</sub> with 9,10-anthracenediylbis(methylene)dimalonic acid (AMDA)<sup>20</sup> (Scheme 3) was adopted to measure the relative <sup>1</sup>O<sub>2</sub> quantum yields of the synthesized porphyrins in PBS (5 mM, pH = 7.0) containing 25% DMSO. The process was similar to DPBF method, except that a medium pressure sodium lamp (500 W, with cut off glass filter λ > 550 nm) in a “merry-go-round” apparatus was used as irradiation light source and the consumption of AMDA was followed by monitoring its absorbance decrease at 380 nm.

### Triplet excited state lifetime

The lifetime of the triplet excited-state was measured using an Edinburgh LP920 laser flash photolysis spectrometer. The third harmonic output (λ = 355 nm, 5 ns of fwhm) of a Nd:YAG laser was used as the excitation source, and a pulsed flashlamp (Xe 900) was used as the analyzing light. All samples were degassed with argon for 20 min before each measurement.

### *n*-Octanol/water partition coefficients (log *P*)

The *n*-octanol/water partition coefficients were measured at room temperature following a reported method.<sup>21</sup> Typically, solutions of each porphyrin (100 μM) in equal volumes of 5 mM PBS, pH 7.0 (1 mL) and *n*-octanol (1 mL) were mixed and sonicated for 30 min. After separation by centrifugation, the amounts of porphyrin in each phase were determined after dilution with DMSO by fluorescence intensity at 658 nm (420 nm excitation) on a F-4500 Fluorescence Spectrophotometer (Hitachi, Japan) and the results were the average of three independent measurements.

### Protein photo-degradation

An Oriel 91192 Solar simulator was used as the light source for the irradiation of the proteins and a 550 nm cut-off filter was used to remove the short wavelength light. Each protein sample (2 μM for BSA and 5 μM for Lyso) in a total volume of 200 μL of 5 mM PBS (pH = 7.0) containing 25% DMSO was irradiated for 3 h. Porphyrin concentrations were fixed at 25 μM.

### Protein electrophoresis

SDS/polyacrylamide gel electrophoresis (SDS-PAGE) experiments were performed as reported.<sup>22</sup> After addition of 5 μL loading buffer, 20 μL of irradiated protein samples was steamed in boiling water for 2 min. Gel electrophoresis was run by applying 100 V for about 1.5 h. The gels were then stained with Coomassie Brilliant Blue R-250 solution for 2 h, destained in a mixture of acetic acid, ethanol and water (10:5:85 in volume ratio) overnight, washed with water, and then scanned on a CanoScan LiDE 700F scanner and processed using Adobe Photoshop software.

### EPR measurement

The EPR spectra were recorded at room temperature on a Bruker-ESP-300E spectrometer at 9.8 GHz, X-band with 100 Hz field modulation. Samples were injected quantitatively into quartz capillaries and purged with oxygen for 15 min in dark, respectively, and illuminated in the cavity of the EPR spectrometer with a Nd:YAG laser at 532 nm (5–6 ns of pulse width, 10 Hz of repetition frequency, 30 mJ/pulse energy).

### Absorption and emission measurements of the bound porphyrins

A 2 mL of porphyrin solution (10  $\mu\text{M}$ ) in PBS/DMSO (3 : 1 in volume ratio) was titrated with a protein solution (2 mM in 5 mM PBS, pH = 7.0) and the absorption and fluorescence spectra were recorded after each addition of the protein.

### Protein fluorescence quenching

A 2 mL of BSA or Lyso solution (2  $\mu\text{M}$  in PBS) was titrated by a porphyrin solution ( $10^{-4}$  M in DMSO) and the protein fluorescence was recorded by excitation at 280 nm. The raw fluorescence intensities, the integral of the emission spectrum in the range of 290–420 nm, were corrected with eqn (4) by considering the inner filter effect of porphyrin,<sup>8g</sup> where  $A_{\text{ex}}$  and  $A_{\text{em}}$  are the optical density of porphyrin at the excitation (280 nm) and emission wavelength maximum (345 nm) of protein and  $F_{\text{raw}}$  is the raw emission intensity of the protein. Binding constants were calculated according to the corrected fluorescence quenching data.

$$F_{\text{corr}} = 10^{(A_{\text{ex}} + A_{\text{em}})/2} F_{\text{raw}} \quad (4)$$

### Acknowledgements

We greatly appreciate the financial support from NNSFC (20772133, 20873170) and CAS (KJCX2.YW.H08).

### Notes and references

- (a) E. D. Stenberg and D. Dolphin, *Tetrahedron*, 1998, **54**, 4151–4202; (b) T. J. Dougherty, C. J. Gomer, B. W. Henderson, G. Jori, D. Kessel, M. Korbek, J. Moan and Q. Peng, *J. Natl. Cancer Inst.*, 1998, **90**, 889–905; (c) M. R. Detty, S. L. Gibson and S. Wagner, *J. Med. Chem.*, 2004, **47**, 3897–3915; (d) E. S. Nyman and P. H. Hynninen, *J. Photochem. Photobiol., B*, 2004, **73**, 1–28; (e) A. E. O'Connor, W. M. Gallagher and A. T. Byrne, *Photochem. Photobiol.*, 2009, **85**, 1053–1074.
- J. Moan and K. Berg, *Photochem. Photobiol.*, 1991, **53**, 549–553.
- (a) M. J. Davies, *Biochem. Biophys. Res. Commun.*, 2003, **305**, 761–770; (b) M. J. Davies, *Photochem. Photobiol. Sci.*, 2004, **3**, 17–25; (c) M. Gracanic, C. L. Hawkins, D. I. Pattison and M. J. Davies, *Free Radical Biol. Med.*, 2009, **47**, 92–102.
- (a) B. Magi, A. Ettore, S. Liberatori, L. Bini, M. Andreassi, S. Frosali, P. Neri, V. Pallini and A. D. Stefano, *Cell Death Differ.*, 2004, **11**, 842–852; (b) P. A. Tsaytler, M. C. O'Flaherty, D. V. Sakharov, J. Krijgsveld and M. R. Egmond, *J. Proteome Res.*, 2008, **7**, 3868–3878.
- (a) F. Kratz, *J. Controlled Release*, 2008, **132**, 171–183; (b) M. J. Hawkins, P. Soon-Shiong and N. Desai, *Adv. Drug Delivery Rev.*, 2008, **60**, 876–885.
- R. K. Pandey, S. Constantine, T. Tsuchida, G. Zheng, C. J. Medforth, M. Aoudia, A. N. Kozyrev, M. A. J. Rodgers, H. Kato, K. M. Smith and T. J. Dougherty, *J. Med. Chem.*, 1997, **40**, 2770–2779.
- (a) C. V. Kumar and A. Buranaprapuk, *J. Am. Chem. Soc.*, 1999, **121**, 4262–4270; (b) C. V. Kumar, A. Buranaprapuk, H. C. Sze, S. Jockusch and N. J. Turro, *Proc. Natl. Acad. Sci. U. S. A.*, 2002, **99**, 5810–5815; (c) A. Suzuki, M. Hasegawa, M. Ishii, S. Matsumura and K. Toshima, *Bioorg. Med. Chem. Lett.*, 2005, **15**, 4624–4627; (d) A. Suzuki, K. Tsumura, T. Tsuzuki, S. Matsumura and K. Toshima, *Chem. Commun.*, 2007, 4260–4262.
- (a) M. Beltramini, P. A. Firey, M. A. J. Rodgers and G. Jori, *Biochemistry*, 1987, **26**, 6852–6858; (b) B. M. Aveline, T. Hasan and R. W. Redmond, *J. Photochem. Photobiol., B*, 1995, **30**, 161–169; (c) I. M. Borissevitch, T. T. Tominaga and C. C. Schmitt, *J. Photochem. Photobiol., A*, 1998, **114**, 201–207; (d) S. M. Andrade and S. M. B. Costa, *Biophys. J.*, 2002, **82**, 1607–1619; (e) N. H. Karapetyan and V. N. Masakyan, *Russ. J. Bioorg. Chem.*, 2004, **30**, 172–177; (f) Y.-B. Yin, Y.-N. Wang and J.-B. Ma, *Spectrochim. Acta, Part A*, 2006, **64**, 1032–1038; (g) F. Tian, E. M. Johnson, M. Zammarripa, S. Samsone and L. Brancaloni, *Biomacromolecules*, 2007, **8**, 3767–3778; (h) X.-L. Lu, J.-J. Fan, Y. Liu and A.-X. Hou, *J. Mol. Struct.*, 2009, **934**, 1–8; (i) E. Alarcón, A. M. Edwards, A. Aspée, C. D. Borsarelli and E. A. Lissi, *Photochem. Photobiol. Sci.*, 2009, **8**, 933–943.
- (a) N. Brasseur, R. Langlois, C. L. Madeleine, R. Ouellet and J. E. van Lie, *Photochem. Photobiol.*, 1999, **69**, 345–352; (b) W. M. Sharman, J. E. van Lie and C. M. Allen, *Adv. Drug Delivery Rev.*, 2004, **56**, 53–76; (c) B. Biplab Bose and A. Dube, *J. Photochem. Photobiol., B*, 2006, **85**, 49–55.
- (a) P. Kubát, K. Lang, Jr and P. Anzenbacher, *Biochim. Biophys. Acta, Gen. Subj.*, 2004, **1670**, 40–48; (b) M. Obata, S. Hirohara, K. Sharyo, H. Alitomo, K. Kajiwara, S. Ogata, M. Tanihara, C. Ohtsuki and S. Yano, *Biochim. Biophys. Acta, Gen. Subj.*, 2007, **1770**, 1204–1211; (c) S. Tanimoto, S. Matsumura and K. Toshima, *Chem. Commun.*, 2008, 3678–3680.
- F. L. Rodkey, *J. Biol. Chem.*, 1961, **236**, 1589–1594.
- F. L. Rodkey, *Arch. Biochem. Biophys.*, 1961, **94**, 38–47.
- (a) S. Fery-Forgues and D. Lavabre, *J. Chem. Educ.*, 1999, **76**, 1260–1264; (b) E. Reddi, M. Cecon, G. Valduga, G. Jori, J. C. Bommer, F. Elisei, L. Latterini and U. Mazzucato, *Photochem. Photobiol.*, 2002, **75**, 462–470.
- (a) N. Cauchon, H.-J. Tian, R. Langlois, C. L. Madeleine, S. Martin, H. Ali, D. Hunting and J. E. van Lie, *Bioconjugate Chem.*, 2005, **16**, 80–89; (b) A. Sholto, S.-W. Lee, B. M. Hoffman, A. G. M. Barrett and B. Ehrenberg, *Photochem. Photobiol.*, 2008, **84**, 764–773.
- (a) I. E. Borissevitch, T. T. Tominaga, H. Imasato and M. Tabak, *J. Lumin.*, 1996, **69**, 65–76; (b) F. Ricchelli, D. Stevanin and G. Jori, *Photochem. Photobiol.*, 1988, **48**, 13–18.
- B. Valeur, *Molecular Fluorescence. Principles and Applications*, Wiley Press, NY, 2001, p. 84.
- J. R. Lakowicz and G. Weber, *Biochemistry*, 1973, **12**, 4161–4170.
- F. D'Souza, G. R. Deviprasad, M. E. El-Khouly, M. Fujitsuka and O. Ito, *J. Am. Chem. Soc.*, 2001, **123**, 5277–5284.
- (a) R. H. Young, K. Wehrly and R. L. Martin, *J. Am. Chem. Soc.*, 1971, **93**, 5774–5779; (b) F. Wilkinson, W. P. Helman and A. B. Ross, *J. Phys. Chem. Ref. Data*, 1993, **22**, 113–262.
- N. A. Kuznetsova, N. S. Gretsova, O. A. Yuzhakova, V. M. Negrimovskii, O. L. Kaliya and E. A. Luk'yanets, *Russ. J. Gen. Chem.*, 2001, **71**, 36–41.
- M. Kepczyński, R. P. Pandian, K. M. Smith and B. Ehrenberg, *Photochem. Photobiol.*, 2002, **76**, 127–134.
- H. Schägger and G. Von Jagow, *Anal. Biochem.*, 1987, **166**, 368–379.